Field emission observed from metal-diamond junctions revealed by atomic force microscopy

S. A. Furkert, A. Wotherspoon, and D. Cherns
H.H. Wills Physics Laboratory, University of Bristol, Avon BS8 1TL, United Kingdom

N. A. Fox[a] and G. M. Fuge
School of Chemistry, University of Bristol, Avon BS8 1TS, United Kingdom

P. J. Heard
Interface Analysis Centre, University of Bristol, Avon BS8 8BS, United Kingdom

S. P. Lansley
Department of Electrical and Computer Engineering, University of Canterbury, Christchurch 8140, New Zealand

(Received 28 March 2007; accepted 11 May 2007; published online 14 June 2007)

A noncontact atomic force microscopy technique has been developed that enables sources of field emission to be detected and mapped in an air ambient. Areas as large as 900 μm^2 have been mapped. This new technique enables determination of the location and extent of the emission area on an individual emitting particle. Emission from nanodiamond particles is shown to occur not at the tip of the diamond, but from near the base where it forms a triple junction with the metal substrate. The reported observations should assist exploration of novel methods of controlling electron emission from devices constructed using diamond particles. © *2007 American Institute of Physics*. [DOI: 10.1063/1.2746079]

Carbon-based materials such as carbon nanotubes (CNTs),[1] diamondlike carbon (DLC),[2] and diamond[3] have demonstrated promising electron emission properties. The high current densities and low turn-on voltages reported for these materials make them potentially useful in emissive display technologies such as field emission displays. Emitters composed of carbon often exhibit a low threshold for field emission; additionally, their microstructures encourage electric field enhancement. This letter, which reports the first direct observation of electron field emission from diamond particles using an atomic force microscope, shows that this is not always the case.

In general, field emission depends on electron tunneling through a surface potential barrier. The emission current may be written as

$$I = \left(\frac{a\lambda A F_{\text{local}}^2}{\varphi}\right)\exp\left(-\frac{\mu b \varphi^{3/2}}{F_{\text{local}}}\right), \tag{1}$$

which is a generalized form of the Fowler-Nordheim equation,[4] where I is the emission current in amperes, F_{local} is the local electric field in V m^{-1}, λ and μ are generalized correction factors, and φ is the work function or electron affinity, for metals and semiconductors, respectively, in eV. The universal constants, a and b are given by

$$a = 1.541 \times 10^{-6}\ \text{A eV V}^{-2}, \tag{2}$$

$$b = 6.830 \times 10^{9}\ \text{eV}^{3/2}\ \text{V m}^{-1}, \text{ and} \tag{3}$$

$$F_{\text{local}} = \beta F_{\text{macro}}, \tag{4}$$

where β is the geometric field enhancement factor and F_{macro} is the macroscopic field. For good conductors, i.e., metals, preferential emission is expected from sharp tips, where values of β in the range of 50–500 have been estimated. The situation is more complex for carbon-based sources, where relatively poor conduction is expected to give rise to field penetration and lower values of β at surface features. Previous work has suggested a variety of emission mechanisms in these materials.[5]

Scanning tunneling microscopy (STM), which enables the work function to be profiled on a nanometer scale, has shown that doped diamond nanoparticle emitters emit preferentially from certain crystal faces and has provided some evidence for low or negative electron affinity.[6] This information was obtained by current imaging tunneling spectroscopy (CITS), where evidence for enhanced emission sites at grain boundaries in boron doped diamond, and in DLC films, was attributed to a field enhancement effect at regions of high conductivity due to dopant segregation.[7,8] It has also been predicted that field emission from thin diamond films occurs due to field enhancement at the back metal/diamond contact or at triple junctions between metal, diamond, and the surrounding vacuum.[9] One limitation of the STM/CITS technique is that scanning is limited to relatively small areas, typically 1–2 μm across. Here an alternative technique is described based on atomic force microscopy (AFM) which allows profiling of areas up to 900 μm^2. AFM surface potential mapping is a well established technique.[10] It involves obtaining a tapping mode (topographic) image with a conductive tip, lifting the tip to a set distance (usually in the range of 50–250 nm), and following the height profile previously obtained while applying a small ac signal ($\Delta V_{\text{ac}} \sin(\omega t)$) to the tip. A difference in surface potential (ΔV_{dc}) between the tip and the surface will cause a change in the electrostatic force F felt as a result of this ac signal.[11]

[a]Electronic mail: neil.fox@bris.ac.uk

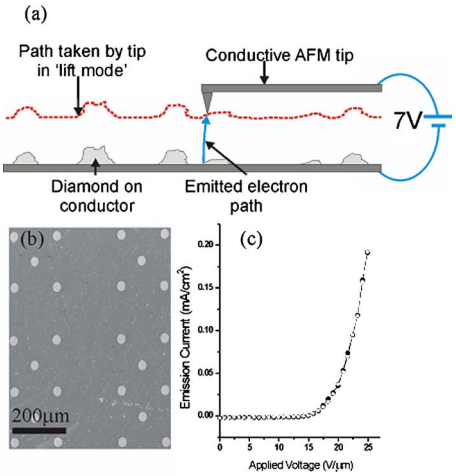

FIG. 1. (Color online) (a) AFM experimental setup for recording field emission from a diamond particle cathode. (b) FIB image showing the emitter structure consisting of lithiated nanodiamond doped Ag dots on a Cr-coated glass substrate and (c) corresponding field emission curve measured at $\sim 1 \times 10^{-8}$ torr.

$$F = \frac{dC}{dz}\Delta V_{\mathrm{dc}}\Delta V_{\mathrm{ac}} \sin(\omega t), \tag{5}$$

where dC/dz is the change of the capacitance C with tip height. In order to counteract the effect of V_{dc}, a bias voltage is applied to the tip until its potential is the same value as that of the surface ($\Delta V_{\mathrm{dc}}=0$). The value of the applied bias is recorded and used to create a map of the surface potential.

An extended surface potential mode is used here to map sites of field emission. Operationally, the main difference is that, after the first surface potential map is obtained, a negative voltage is applied to the sample, as shown in Fig. 1(a). If there are no emission sites, the resulting image will be the same as the standard surface potential map, but with an offset voltage equal to the applied voltage. Any emission sites will be revealed as areas of extremely high surface potential—where the field emission current swamps the feedback current that is used to control the voltage applied to the tip. The electronic feedback circuit responds to the electron emission by attempting to apply a matching bias voltage to the tip. Since the circuit is unable to deliver a value that is large enough, the system response is to represent the area of emission by a maximum in surface potential. The same system response can be observed if the conductive tip is deliberately brought into contact with the surface while a bias is applied to it.

Studies were carried out on diamond field emitters produced by inkjet printing arrays of 30 μm dots containing colloidal Ag and monocrystalline (0.5 μm) diamond onto Cr-coated glass substrates, as detailed in Fig. 1(b). The diamond was lightly predoped with Li using a patented process.[12] A lithium concentration of 6×10^{19} at. cm^{-3} was determined by secondary ion mass spectroscopy, using a gallium ion source. The material had a room temperature mobility of 5 $\mathrm{cm}^2/\mathrm{V\,s}$, a bulk resistivity of 0.139 Ω cm, a carrier concentration of 9×10^{18} cm^{-3}, and a negative Hall coefficient of 0.67 $\mathrm{m}^2\,\mathrm{C}^{-1}$. Following an air bake at 150 °C for 30 min, the dot array was ablated in air (ArF excimer laser, 193 nm), which served to remove Ag nanoparticles on the protruding surfaces of the diamond. Removal of Ag nanoparticles was observed using a focused ion beam (FIB) microscope. Macroscopic *I-V* curves typical of field emission were obtained from the dot array using a vacuum diode with a 300 μm anode to cathode gap. A threshold voltage of 15 $\mathrm{V}/\mu\mathrm{m}$ was recorded at a current density of 7×10^{-4} $\mathrm{mA/cm}^2$ [Fig. 1(c)].

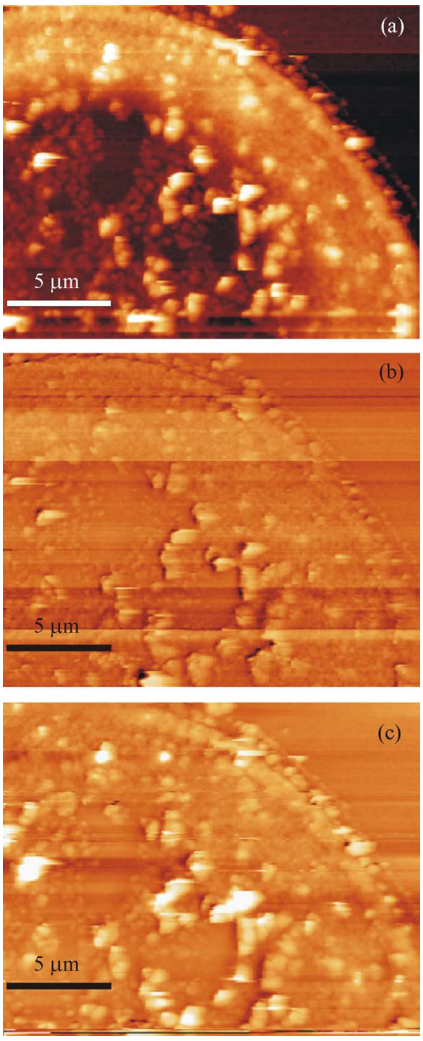

FIG. 2. (Color online) 25×20 $\mu\mathrm{m}^2$ images of part of a single dot. (a) Height profile. [(b) and (c)] Surface potential maps using, respectively, 0 V (a) and −9 V (b) potential difference between the surface and tip, illustrating field emission from particles with an emitter site density higher than 10^7 sites/cm^2.

Arrays were then examined by AFM using a Veeco Instruments Dimension 3100 AFM with a Nanoscope IV controller. Figure 2 shows typical results, taken from part of a single ablated silver dot incorporating diamond particles. Figure 2(a) shows the topology scan, in which individual diamond particles, or agglomerates of a few particles, appear as brighter (i.e., higher) features. Figure 2(b) shows a surface potential scan at zero bias, revealing the difference in surface potential between the diamond particles and the surrounding metal back contact. Figure 2(c) shows a surface potential map taken with $V_{\mathrm{dc}}=-9$ V bias applied to the sample. In this case some, but not all, diamond particles are emitting, as shown by the white areas on the map.

The advantage of this mapping technique is that it enables the exact location of emitter sites to be quickly determined, without damaging the sample. Being able to show the proportion of potential emission sites that are emitting can help to establish the causes of nonuniformity over large areas

of emitters. By repeating a scan of the same area many times over a number of hours, information on the uniformity and operational stability of individual emitters can be recorded. While the image is being mapped the bias voltage applied to the sample can be varied, allowing individual emission sites to be turned on and off while scanning. Knowledge of the bias needed to turn on an emitter enables the threshold voltage for an emission site to be determined and, if desired, compared to the neighboring emission sites. This also allows examination of the effect of higher field strengths on emission site performance, revealing whether increased field strengths cause an increase in the number of emission sites or simply cause the existing sites to emit more strongly. For the doped nanodiamonds imaged in this study, the latter was the case. The approximate turn-on voltage for field emission from the diamond emitters detailed in Fig. 2, was 20 V/μm. This is of the same order of magnitude as the macroscopic threshold field measured using a large area cathode of the same material operated in a demountable vacuum diode test station.

It has long been assumed that the main effect controlling field emission is geometric field enhancement.[13] Nanotip emitters that rely on geometric field enhancement such as CNTs generally require an exclusion zone of several microns[14] around each emitter, to prevent their emission property being quenched due to electrostatic screening effects. Even in cases where the emitter is flat, such as DLC films, it has been claimed that emission originates from small areas of high conductivity that caused areas of local field enhancement, or "virtual tips."[15]

Establishing whether emission originates from the highest point or from another region on the emitter surface can yield important information on the surface property of the emitter particle. This AFM technique allows the exact position of emission to be determined because it is able to examine emission sites on a nanometre scale. When a single emitting diamond was mapped, it was discovered that the emission did not originate from the tip, where the greatest electric field would be expected, but from the sides near its connection to the metal substrate. This was the case for all the diamond emitters examined, as illustrated in Fig. 3. In order to ensure that the results were not caused by artifacts generated by the variable thickness of the metal film surrounding the diamond, an AFM tip was used to create ridges in the metal that were equal or greater in height than the emission sites and had a similar profile. These did not emit, thereby confirming that the diamond was the cause of the electron emission and not local field enhancement from the metal profile. This study thus provides the first direct evidence that the emission is dependent on the triple junction between the metal back contact, diamond, and air (vacuum).

It is suggested that the electrons first tunnel from the metal into the conduction band of the diamond. Li doping is believed to produce a *n*-type region near the diamond surface, which should minimize the width of the potential barrier through which tunneling occurs.[16,17] Once injected into the diamond, electrons which reach the surface ballistically, i.e., without being scattered, will have a high chance of being emitted owing to the low, or even negative, electron affinity of the diamond surface.

In summary, electron emission from a lithium-doped diamond particulate emitter is dependent on the triple junction between the metal back contact, diamond, and air/vacuum rather than on the diamond particle topology. The results presented in this letter could have significant implications for the design of large area, low cost emitter cathodes based on conducting diamond particles. As geometric field enhancement does not play a significant part in determining which particles emit, the nanodiamonds can be more closely packed and their dimensions tailored to optimize emission.

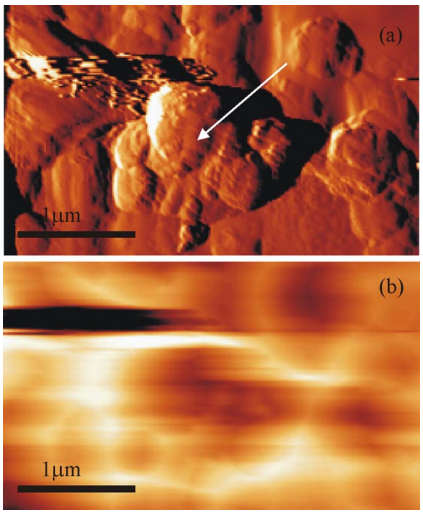

FIG. 3. (Color online) (a) Height profile of a particle cluster with the arrow highlighting the largest. (b) Surface potential map when a −7.5 V bias voltage is applied to the sample. The emission shows up as white areas around the periphery of the diamond.

The authors are grateful to M. N. R. Ashfold and Keith Rosser (Chemistry) and Richard Exley (Physics) for their many and varied contributions to this work. The authors would also like to thank M. J. Miles (Physics) for access to the AFM equipment used in this work. This work was financially supported in part by Advance Nanotech Ltd.

[1] W. A. de Heer, A. Chatelain, and D. Ugarte, Science **270**, 1179 (1995).
[2] G. A. J. Amaratunga and S. R. P. Silva, Appl. Phys. Lett. **68**, 2529 (1996).
[3] W. Zhu, G. P. Kochanski, S. Jin, and L. Seilbles, J. Appl. Phys. **78**, 2707 (1995).
[4] R. G. Forbes, J. Vac. Sci. Technol. B **17**, 526 (1999).
[5] J. Robertson, Mater. Res. Soc. Symp. Proc. **509**, 83 (1998).
[6] W. N. Wang, N. A. Fox, J. W. Steeds, and J. E. Butler, J. Appl. Phys. **80**, 6809 (1996).
[7] H.-F. Cheng, Y.-C. Lee, S.-J. Lin, Y.-P. Chou, T. T. Chen, and I.-N. Lin, J. Appl. Phys. **97**, 044312 (2005).
[8] G. A. J. Amaratunga, M. Baxendale, N. Rupesinghe, I. Alexandrou, M. Chhowalla, T. Butler, A. Munindradasa, C. J. Kiley, L. Zhang, and T. Sakai, New Diamond Front. Carbon Technol. **9**, 31 (1999).
[9] M. W. Geis, N. N. Efremow, Jr., K. E. Krohn, J. C. Twichell, T. M. Lyszczarz, R. Kalish, J. A. Greer, and M. D. Taber, Nature (London) **393**, 431 (1998).
[10] L. Zhang, T. Sakai, N. Sakuma, and T. Ono, Jpn. J. Appl. Phys., Part 1 **39**, 3728 (2000).
[11] Veeco Application note AN27 for Dimension 3100.
[12] Patent Aapplication No. PCT/GB2004/003696 (29 August 2004).
[13] Vu Thien Binh and S. T. Purcell, Appl. Surf. Sci. **111**, 157 (1997).
[14] L. Nilsson, O. Groening, C. Emmenegger, O. Kuettel, E. Schaller, L. Schlapbach, H. Kind, J.-M. Bonard, and K. Kern, Appl. Phys. Lett. **76**, 2071 (2000).
[15] O. Gröning, O. M. Küttel, P. Gröning, and L. Schlapbach, Appl. Phys. Lett. **71**, 2253 (1997).
[16] M. W. Geis, J. C. Twichell, and T. M. Lyszczarz, J. Vac. Sci. Technol. B **14**, 2060 (1996).
[17] M. S. Chung, S. C. Hong, P. H. Cutler, N. M. Miskovsky, B. L. Weiss, and A. Mayer, J. Vac. Sci. Technol. B **24**, 909 (2006).